Combined Kinetic Analysis of Solid-State Reactions: A Powerful Tool for the Simultaneous Determination of Kinetic Parameters and the Kinetic Model without Previous Assumptions on the Reaction Mechanism

L. A. Pérez-Maqueda,* J. M. Criado, and P. E. Sánchez-Jiménez

Instituto de Ciencia de Materiales de Sevilla, C.S.I.C.-Universidad de Sevilla, C. Americo Vespucio no 49, 41092 Sevilla, Spain

Received: July 27, 2006; In Final Form: September 14, 2006

The combined kinetic analysis implies a simultaneous analysis of experimental data representative of the forward solid-state reaction obtained under any experimental conditions. The analysis is based on the fact that when a solid-state reaction is described by a single activation energy, preexponetial factor and kinetic model, every experimental $T-\alpha-d\alpha/dt$ triplet should fit the general differential equation independently of the experimental conditions used for recording such a triplet. Thus, only the correct kinetic model would fit all of the experimental data yielding a unique activation energy and preexponential factor. Nevertheless, a limitation of the method should be considered; thus, the proposed solid-state kinetic models have been derived by supposing ideal conditions, such as unique particle size and morphology. In real systems, deviations from such ideal conditions are expected, and therefore, experimental data might deviate from ideal equations. In this paper, we propose a modification in the combined kinetic analysis by using an empirical equation that fits every $f(\alpha)$ of the ideal kinetic models most extensively used in the literature and even their deviations produced by particle size distributions or heterogeneities in particle morphologies. The procedure here proposed allows the combined kinetic analysis of data obtained under any experimental conditions without any previous assumption about the kinetic model followed by the reaction. The procedure has been verified with simulated and experimental data.

Introduction

The kinetics of solid-state reactions is generally described, when data are recorded under experimental conditions far from equilibrium, by two functions, one, $f(T)$, accounts for the temperature, T, dependence, and the other, $f(\alpha)$, accounts for the conversion, α, dependence. $f(T)$ is expressed by an Arrhenius-type equation, and $f(\alpha)$ is an algebraic expression usually associated with a physical model that describes the kinetics of the solid-state reaction. A list of the most commonly used kinetic models is shown in Table 1. These physical models have been proposed by assuming a driving force, i.e., interface growth, diffusion, nucleation-growth, and a simplified and homogeneous geometry.[1−4]

The scope of the kinetic analysis of a thermally stimulated solid-state reaction is the discrimination of both $f(T)$ and $f(\alpha)$ from experimental data. Several procedures have been proposed in the literature for the kinetic analysis of experimental data obtained under different temperature evolution conditions, i.e., isothermal, linear heating rate, modulated temperature, sample controlled. Most of the different kinetic analysis procedures are intended to be used for the analysis of experimental data obtained under determined experimental conditions.[1,5−11] Recently, we proposed a kinetic analysis procedure that allows the combined analysis of a set of data obtained under different experimental conditions.[12−15] The procedure is based on the fact that only the true kinetic model fits simultaneously all experimental data yielding an unique $f(T)$ function. This procedure has been successfully applied to the combined study of data obtained under different experimental conditions, such as isothermal, linear heating or sample controlled, for both crystallization and thermal decomposition of solids.

The problem arises when the process cannot be described by one of the $f(\alpha)$ functions proposed for the study of solid-state reactions. These functions are, as stated above, algebraic expressions of simplified physical models that assume, for example, that the system has a simple and homogeneous geometry. In many real systems, it is expected a deviation of such simplified physical models due to heterogeneity in the samples. The influence of heterogeneity in kinetic analysis has been already pointed out in the literature.[16−21] Thus, it has been reported that a particle size distribution instead of a unique particle size produces a decrease in the ability to discriminate the geometry of the reaction interface.[17] These deviations from the ideal models imply a limitation in the kinetic analysis because none of the $f(\alpha)$ equations already proposed will properly fit all of experimental data. In principle, this limitation could be overcome by increasing the list of models with new ones that account for some of these deviations from ideal situations. Nevertheless, this solution is not practical because the number of possible models will eventually be infinite. An alternative solution is the use of a fitting function for $f(\alpha)$ that behaves like an umbrella that covers any of the kinetic functions that would describe a solid-state reaction. Thus, when analyzing real data, the analysis will not be limited by a restricted list of models. In this paper, we propose the use of the combined kinetic analysis, which allows analyzing data obtained under any experimental conditions, with a general fitting function for $f(\alpha)$. Different deviations from ideal situations produced by

* Corresponding author. E-mail: maqueda@cica.es.

10.1021/jp064792g CCC: $33.50
Published on Web 10/21/2006

TABLE 1: Algebraic Expressions for the $f(\alpha)$ Functions for the Most Common Mechanisms in Solid-State Reactions and Their Corresponding Equivalent Reduced Sestak−Berggren Equations

mechanism	symbol	$f(\alpha)$	equivalent reduced Sestak−Berggren equation
phase boundary controlled reaction (contracting area, i.e., bidimensional shape)	R2	$(1-\alpha)^{1/2}$	$(1-\alpha)^{1/2}$
phase boundary controlled reaction (contracting volume, i.e., tridimensional shape)	R3	$(1-\alpha)^{2/3}$	$(1-\alpha)^{2/3}$
unimolecular decay law (instantaneous nucleation and unidimensional growth)	F1	$(1-\alpha)$	$(1-\alpha)$
random instant nucleation and two-dimensional growth of nuclei (Avrami−Erofeev equation)	A2	$2(1-\alpha)[-\ln(1-\alpha)]^{1/2}$	$2.079(1-\alpha)^{0.806}\alpha^{0.515}$
random instant nucleation and three-dimensional growth of nuclei (Avrami−Erofeev equation)	A3	$3(1-\alpha)[-\ln(1-\alpha)]^{2/3}$	$3.192(1-\alpha)^{0.748}\alpha^{0.693}$
two-dimensional diffusion (bidimensional particle shape)	D2	$1/[-\ln(1-\alpha)]$	$0.973(1-\alpha)^{0.425}\alpha^{-1.008}$
three-dimensional diffusion (tridimensional particle shape) Jander equation	D3	$[3(1-\alpha)^{2/3}]/\{2[1-(1-\alpha)^{1/3}]\}$	$4.431(1-\alpha)^{0.951}\alpha^{-1.004}$

particle size distributions, changes in interface morphology, etc. would be analyzed. Finally, the proposed procedure is tested for the analysis of simulated and experimental data.

Theoretical

The reaction rate, $d\alpha/dt$, of a solid-state process can be related to the process temperature, T, and to the reacted fraction, α, by means of the following general equation:

$$\frac{d\alpha}{dt} = A\exp(-E/RT)f(\alpha) \tag{1}$$

where A is the Arrhenius preexponential factor, R is the gas constant, and E is the activation energy. In a thermo-analytical experiment, the sample is heated while the evolution of the reacted fraction, or reaction rate, is recorded as a function of time and temperature. For the experiments, different heating pathways can be used, the most common ones being isothermal, linear heating, modulated temperature, and sample-controlled. In the isothermal experiment, sample is rapidly heated to a certain temperature and maintained constant along the entire experiment. Thus, the term $A\exp(-E/RT)$, usually referred as k, is constant. Therefore, eq 1 can be written as follows:

$$\frac{d\alpha}{dt} = kf(\alpha) \tag{2}$$

eq 2 can be integrated to give

$$\int_0^\alpha \frac{d\alpha}{f(\alpha)} = A\exp(-E/RT)\int_0^t dt \tag{3}$$

or

$$g(\alpha) = kt \tag{4}$$

Under other experimental conditions, such as linear heating rate, the temperature is linearly raised with the time. Thus, the heating rate, β, is defined by the following equation:

$$\beta = \frac{dT}{dt} \tag{5}$$

and under these experimental conditions, eq 1 can be written as follows:

$$\frac{d\alpha}{dT} = \frac{A}{\beta}\exp(-E/RT)f(\alpha) \tag{6}$$

or in its integral form:

$$g(\alpha) = \frac{A}{\beta}\int_0^T \exp(-E/RT)\,dT \tag{7}$$

The integral in the right-hand side term cannot be written in a closed form and it has to be numerically solved or approached using one of the approximated equations proposed in the literature.

A recently proposed modification of the linear heating rate program is the modulated temperature program, where a sinusoidal temperature modulation is superimposed to the linear heating rate program.[22−24] Therefore, the heating rate is defined as follows:

$$\beta = \beta_0 + B\sin(\varpi t) \tag{8}$$

where β_0 is the constant heating rate, B is the amplitude of the modulation, and ω is the frequency.

In the sample-controlled thermal analysis experiment (SCTA), the evolution of the reaction rate with the time is predefined by the user.[25,26] Usually, the reaction rate is maintained constant along the entire process, although other profiles, such as linear evolution with time, have been also proposed.[27−29] In the most common case

$$\frac{d\alpha}{dt} = C \tag{9}$$

where C is the selected constant rate. Thus, eq 1 can be written

$$C = A\exp(-E/RT)f(\alpha) \tag{10}$$

The four heating procedures described above are the most common ones, but others have been proposed and in some cases implemented in commercial thermo-analytical instruments. For each of these heating procedures, different specific kinetic analysis methods have been reported. Nevertheless, as stated above every resulting triplet $\alpha-d\alpha/dt-T$ recorded under any experimental conditions should fit eq 1 or its logarithmic form, which can be written as follows:

$$\ln\left(\frac{d\alpha/dt}{f(\alpha)}\right) = \ln A - E/RT \tag{11}$$

because this equation does not imply any consideration about the heating pathway. Besides, the plot of the left-hand side of eq 11 versus the inverse of temperature yields a straight line if the correct $f(\alpha)$ function is considered. From this plot, the activation energy can be obtained from the slope, and the

preexponential factor is obtained from the intercept. Nevertheless, we have to take into consideration some limitations. Thus, it is known that under linear heating rate conditions, it is not possible to discriminate the dependence of temperature and reacted fraction on the reaction rate from a single experimental curve, because a single curve could be fitted by more than one $f(\alpha)$ function and the resulting $f(T)$ function will drastically depend on the selected $f(\alpha)$.[5,13,30,31] Therefore, to discriminate the correct kinetic parameters, several experimental curves obtained under different experimental condition, such as different linear heating rates, should be simultaneously analyzed. Another limitation is related with the fact that the $f(\alpha)$ functions proposed in the literature are, as stated in the Introduction section, idealized physical models that, although having successfully described many real systems, might not be used for every solid-state process. To overcome this restriction, we propose the use of the following algebraic expression for $f(\alpha)$:

$$f(\alpha) = (1 - \alpha)^n \alpha^m \tag{12}$$

This equation is a simplified form of the Sestak−Berggren equation:[32]

$$f(\alpha) = (1 - \alpha)^n \alpha^m (-\ln(1 - \alpha))^p \tag{13}$$

for $p = 0$. The Sestak−Berggren kinetic equation, unlike those in Table 1, is an empirical equation without physical meaning. Nevertheless, we have observed that this function exactly matches any of the functions in Table 1 after introducing the accommodation constant c in eq 12 that becomes

$$f(\alpha) = c(1 - \alpha)^n \alpha^m \tag{14}$$

The resulting c, n, and m parameters have been calculated by fitting the different $f(\alpha)$ functions with eq 14; the corresponding equivalent functions describing the different ideal kinetic models are shown in Table 1. The $f(\alpha)$ versus α plots together with the Sestak−Berggren equation with the corresponding c, n and m parameters are represented in Figure 1. It is quite evident from plots in Figure 1 that the fitting is excellent. Therefore, eq 12 can describe every kinetic model in Table 1 just by selecting the proper c, n and m parameters.

From eq 11 and 14, the following equation can be written, which should fit every experimental data:

$$\ln\left(\frac{d\alpha/dt}{(1 - \alpha)^n \alpha^m}\right) = \ln cA - E/RT \tag{15}$$

The method proposed here for determining the kinetic parameters is a multistage procedure. First, the Pearsons linear correlation coefficient between the left-hand side of eq 15 and the reciprocal of temperature is used as the objective function for optimization, where n and m are the variable parameters to maximize the objective function. Here, optimization has been performed by means of the maximize function of Mathcad software (Mathsoft inc.). By this optimization procedure, the n and m parameters that yield the best linear correlation for the plot of the left-hand side of eq 15 versus the reciprocal of temperature are obtained. Then, the real activation energy is obtained from the slope of the plot of the left-hand side of eq 15 versus the reciprocal of temperature and the preexponential factor multiplied by the factor c is obtained from the intercept. It should be noted that although we propose the use of the simplified Sestak−Berggren equation (eq 14), identical results are obtained from different equations if these equations fit all of the equations corresponding to ideal models tabulated in Table 1. Nevertheless, we proposed the simplified Sestak−Berggren equation because it is quite a simple equation and is extensively used in solid-state kinetics. The kinetic analysis method here outlined will be tested in the next section with different sets of both simulated and experimental curves.

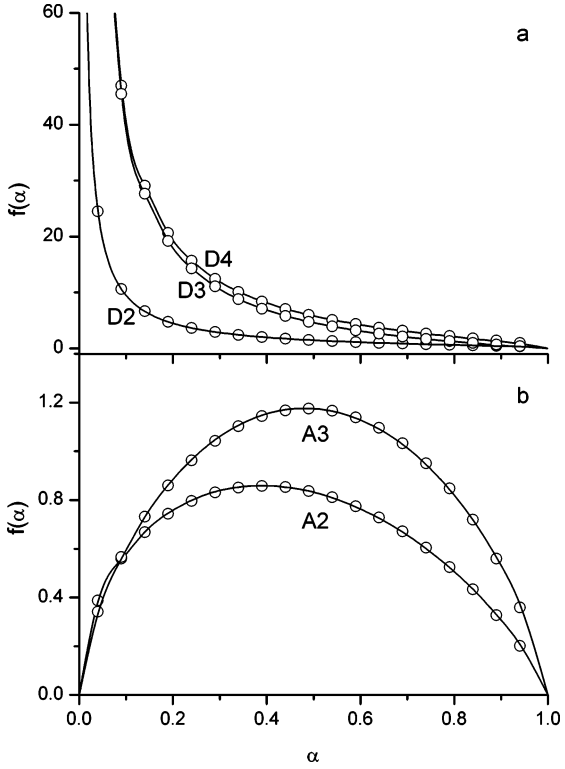

Figure 1. Comparison of the $f(\alpha)$ (dots) corresponding to diffusion (a) and nucleation−growth (b) mechanisms with the Sestak−Berggren equations with the corresponding n and m parameters tabulated in Table 1 (solid lines).

Results

Figure 2 shows a set of curves simulated for a solid-state reaction that follows an A3 kinetic model with an activation energy of 175 kJ mol^{-1} and a preexponential factor of 10^{13} min^{-1}. Curves have been simulated for isothermal (T = 625 °C, curve a), linear heating (heating rates, β = 2, 5, 10 °C min^{-1}), sample controlled thermal analysis (reaction rate, $C = 10^{-1}$ min^{-1}) and modulated temperature conditions (constant heating rate, β_0 = 5 °C min^{-1}; frequency, ω = 2 min^{-1}; amplitude of the modulation, B = 2 °C). All of these four curves have been simultaneously analyzed by eq 15, yielding a perfect straight line (Figure 3), with a correlation factor of 1, for the n and m parameters obtained by the optimization procedure described above, i.e., $n = 0.748$ and $m = 0.693$. Moreover, the activation energy, 175 kJ mol^{-1}, obtained from the slope is identical to that used for the simulation, and the value of the intercept, 3.192×10^{13}, corresponds to cA. Similar results have been obtained from simulated curves for all the kinetic models shown in Table 1, but they have been omitted by the sake of brevity.

It is noteworthy to point out that the simultaneous determination of the kinetic parameters and the $f(\alpha)$ function from eq 15 necessarily requires the combined analysis of a set of different $\alpha-T$ (or t) plots. It does not work for instance with a single TG curve obtained under a linear heating program because other kinetic models besides the real one obeyed by the reaction would fit this curve while leading to wrong kinetic parameters.

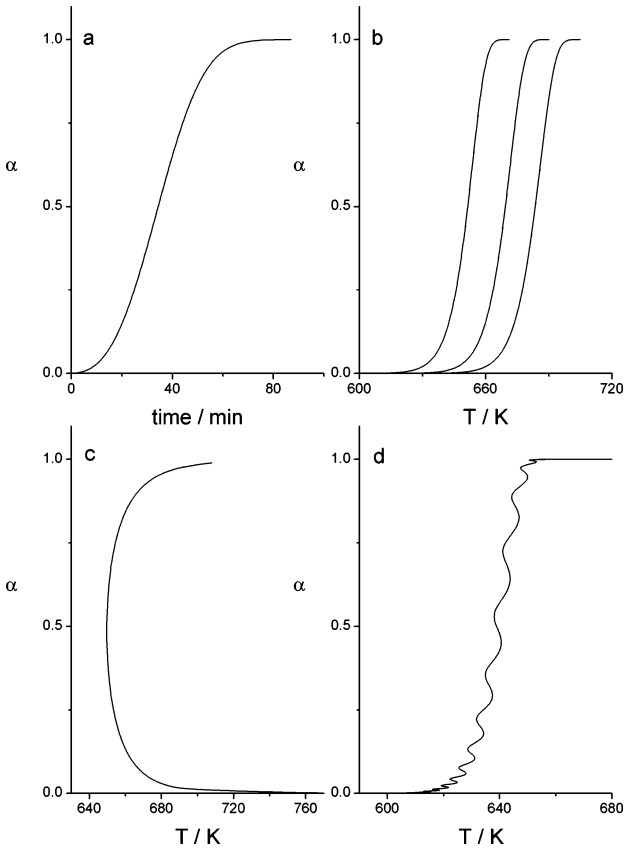

Figure 2. Simulated curves assuming an A3 kinetic model, an activation energy of 175 kJ mol^{-1} and a preexponential factor of 10^{13} min^{-1} and the following conditions: (a) isothermal (T = 625 °C), (b) linear heating (heating rate, β = 2, 5, 10 °C min^{-1}), (c) sample controlled thermal analysis (constant reaction rate, $C = 10^{-1}$ min^{-1}, curve c), and (d) modulated temperature conditions (constant heating rate, β_0 = 5 °C min^{-1}; frequency, ω = 2 min^{-1}; amplitude of the modulation, B = 2 °C).

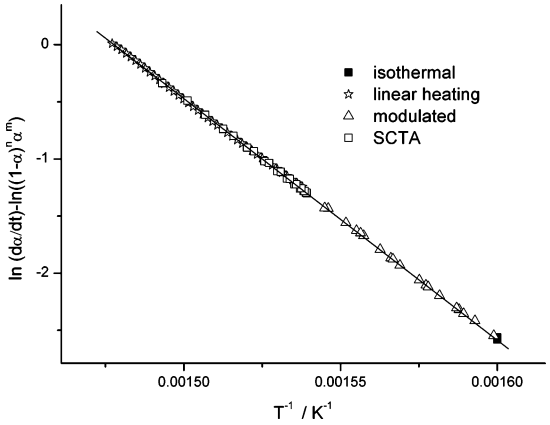

Figure 3. Combined analysis of curves included in Figure 2 by means of eq 15 for the n and m parameters obtained by the optimization procedure, i.e., n = 0.748 and m = 0.693.

Thus, Figure 4 shows that the TG diagrams included in Figure 2b can be individually fitted by a first-order kinetic model with a regression coefficient r = 1, despite having been simulated for an A3 kinetic model. However, the plot of the whole set of TG data according to eq 15 does not yield a single straight line, as that shown in Figure 4, but a set of three parallel plots corresponding to every α−T plot included in Figure 2b. Moreover, an activation energy of 521 kJ.mol^{-1} results from the slopes of the three lines in Figure 3, which is quite different from the value used for the simulations (E = 175 kJ·mol^{-1}).

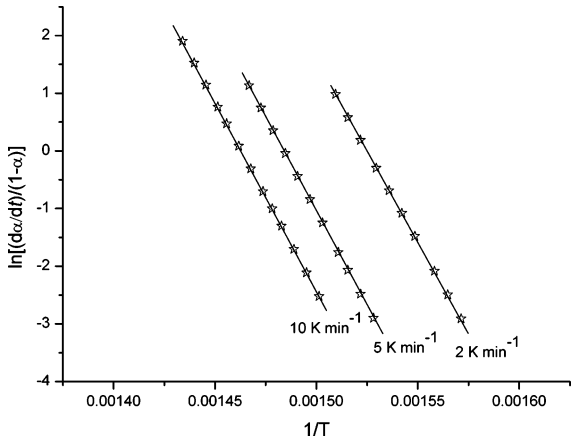

Figure 4. Analysis of the α−T plots included in Figure 2b according to eq 15 by assuming a F1 kinetic model [i.e. $f(\alpha) = (1 - \alpha)$].

It was mentioned above that the method here proposed could be used to analyze curves even when the $f(\alpha)$ function is not described by one of the ideal models included in Table 1. Thus, to test this possibility, a set of curves have been simulated using the procedure described in ref 17 assuming a log-normal particle size distribution:

$$\frac{d\phi}{dz} = \frac{1}{\sigma\sqrt{2\pi}} \exp\left(-\frac{(z-\bar{z})^2}{2\sigma^2}\right) \qquad (16)$$

where ϕ is the frequency, σ is the standard deviation in logarithmic scale, and z *is* the particle size in logarithmic scale. For the different kinetic models, the particle size will have a different meaning. Thus, for R3, D3 and D4, the size will be the sphere diameter, and for R2 and D2, it will be the base diameter of the cylinder. For the simulation, the distribution curve is divided into 400 equal slices, parallel to the vertical axis. For each of these slices, a simulated curve is obtained from eq 1 considering the particle size dependence for the considered mechanism. Finally, the overall α versus T curve is determined by adding all of the individual curves corresponding to the different slices. The resulting curves simulated for a D_2 kinetic model under linear heating rate conditions assuming particle size distribution (σ = 0.75) an activation energy of 100 kJ mol^{-1} and a preexponential factor of 10^5 min^{-1} are included in Figure 5. The analysis of curves in Figure 5 by means of eq 15 yields a straight line for n = 0.93466 and m = −0.82728 (Figure 6) with a correlation coefficient of 1, and the resulting activation energy, as obtained from the slope, is 100 kJ mol^{-1} and the intercept is 1.9×10^4. Simulated curves were reconstructed by using the kinetic parameters resulting from the analysis (both sets of curves are included in Figure 5); it is clear from this figure that both sets of curves are superimposed, verifying the proposed kinetic analysis procedure.

Another possible deviation from ideal models might be produced if particles in the material are not homogeneous in shape. It was mentioned above that the ideal models have been proposed by assuming specific geometries, such as spheres, cylinders or planes, that might be different from those in the real samples. Additionally, in many real samples, shape heterogeneity is expected. Figure 7 includes a set of linear heating rate curves that have been simulated by assuming that the sample is constituted by two different kinds of particles, i.e., spherical (75%) and cylindrical (25%), whose decompositions follow interface controlled kinetic models (R3 and R2, respectively) with a unique activation energy (E = 100 kJ mol^{-1})

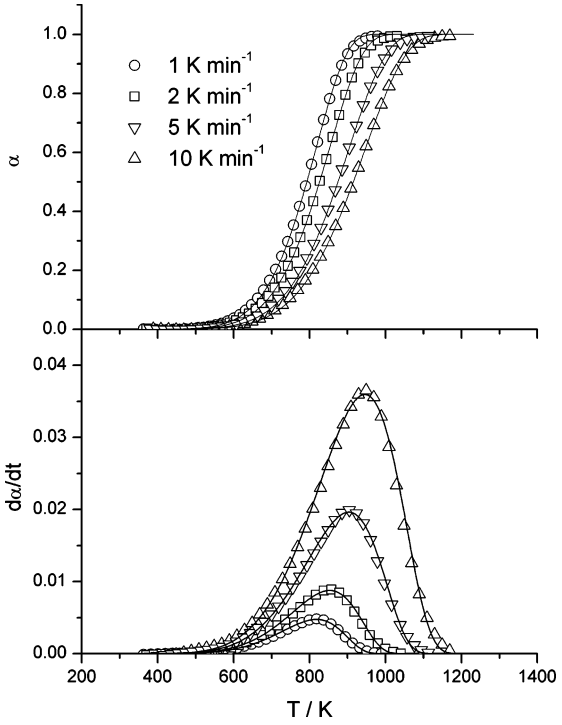

Figure 5. Simulated curves (dots) under linear heating rate conditions assuming particle size distribution ($\sigma = 0.75$) an activation energy of 100 kJ mol^{-1} and a preexponential factor of 10^5 min^{-1}. Curves reconstructed with the kinetic parameters resulting from the combined kinetic analysis are also plotted (solid lines).

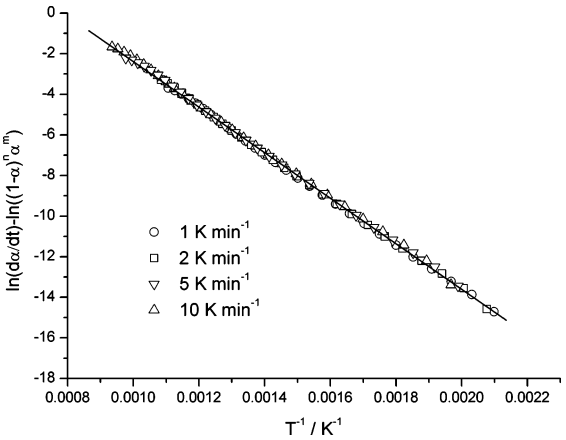

Figure 6. Combined analysis of curves included in Figure 5 by means of eq 15 for the *n* and *m* parameters obtained by the optimization procedure, i.e., $n = 0.934\,66$ and $m = -0.827\,28$.

and preexponential factor ($A = 10^{10}$ min^{-1}). The analysis of these curves by means of eq 15 yields a straight line for $n = 0.637\,019\,19$ and $m = 0.006\,980\,94$ (Figure 8) with a correlation coefficient of 1. The activation energy and preexponential factor obtained from the slope and intercept, respectively, are coincident with those used for the simulation. Therefore, it has been shown that the kinetic analysis procedure proposed here allows analyzing data even when the process cannot be described by one of the ideal models due heterogeneity in, for example, particle shape or size, yielding the correct kinetic parameters.

Once the method has been tested from theoretical curves, it is of interest to verify it with experimental curves. Thus, the kinetics of the thermal decomposition of a barium carbonate sample has been chosen because this reaction has been previously studied by us, and its kinetics is well described.[33] For this reaction, experiments under sample controlled thermal

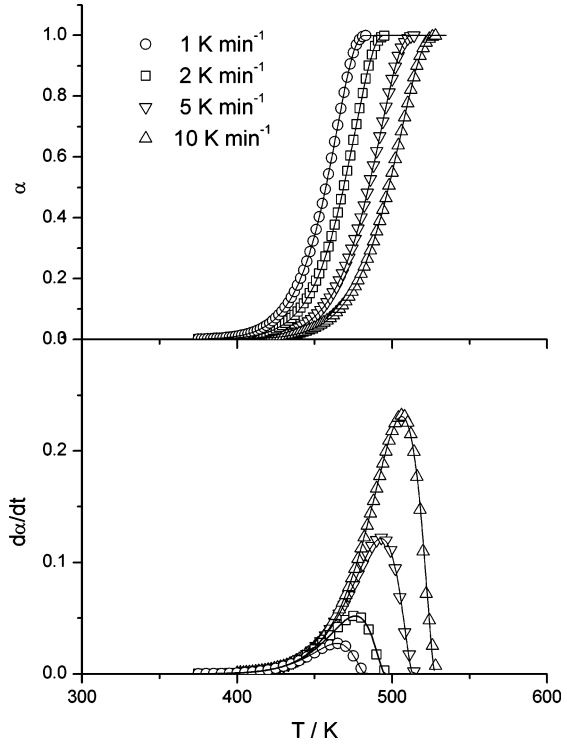

Figure 7. Linear heating rate curves (dots) simulated by assuming that the sample is constituted by two different kinds of particles, i.e., spherical (75%) and cylindrical (25%), whose decompositions follow interface controlled kinetic models (R3 and R2, respectively) with a unique activation energy ($E = 100$ kJ mol^{-1}) and preexponential factor ($A = 10^{10}$ min^{-1}). Curves reconstructed with the kinetic parameters resulting from the combined kinetic analysis are also plotted (solid lines).

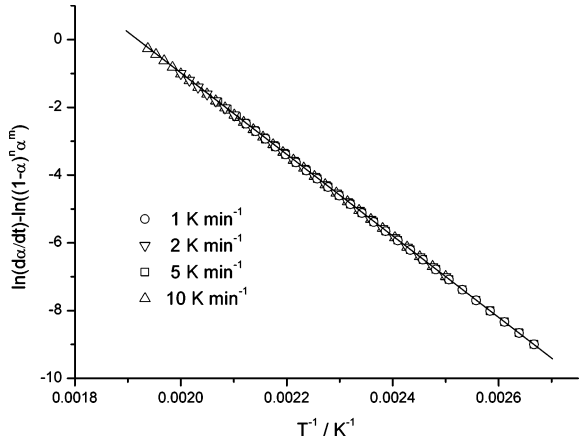

Figure 8. Combined analysis of curves included in Figure 7 by means of eq 15 for the *n* and *m* parameters obtained by the optimization procedure, i.e., $n = 1.081$ and $m = -0.0246$.

analysis and linear heating rate conditions were recorded.[33] The resulting $\alpha - T$ curves are included in Figure 9 and the experimental conditions are described in the figure caption. The combined kinetic analysis of these two curves by means of the procedure described above yields a straight line for $n = 1.081$ and $m = -0.0246$ (Figure 10) with a correlation coefficient of 0.999, resulting in an activation energy, as obtained from the slope, of 225 ± 2 kJ mol^{-1} and a preexponetial factor, as obtained from the intercept, of $(9.6 \pm 1) \times 10^6$ min^{-1}. The normalized Sestak−Berggren function with the resulting values of *n* and *m* coefficients is represented in Figure 11 as a function of α together with the $f(\alpha)$ functions corresponding to some of the ideal models included in Table 1. It can be observed from

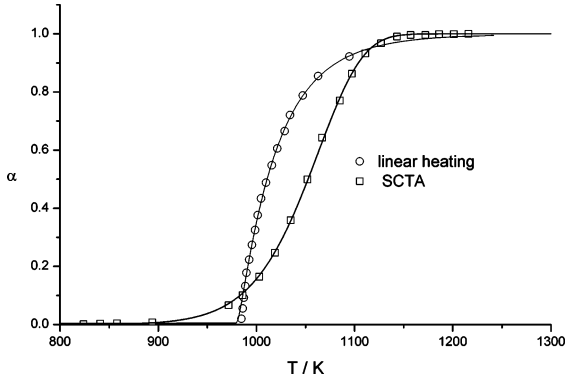

Figure 9. Experimental curves obtained for the thermal decomposition of a $BaCO_3$ sample under a vacuum at constant decomposition rate $C = 6 \times 10^{-4}$ min^{-1} (○) and a linear heating rate $\beta = 0.2$ K min^{-1} (□). Reconstructed curves using the kinetic parameters resulting of the combined kinetic analysis are plotted as solid lines.

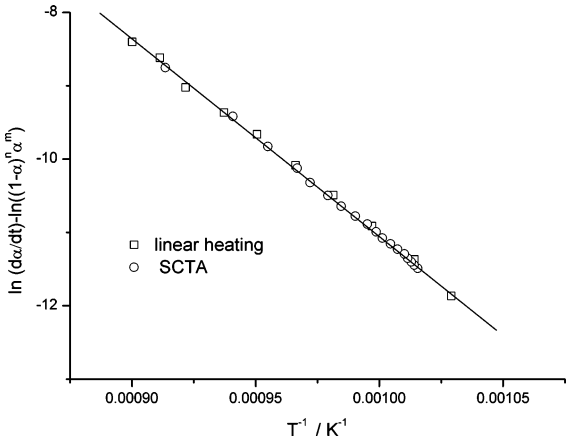

Figure 10. Combined analysis of experimental curves included in Figure 9 by means of eq 15 for the *n* and *m* parameters obtained by the optimization procedure, i.e., $n = 1.081$ and $m = -0.0246$.

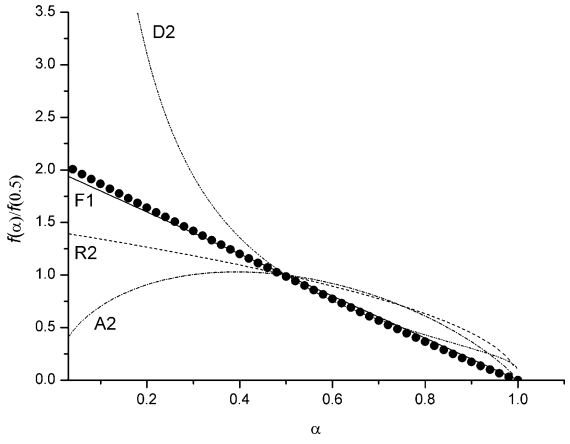

Figure 11. Comparison of the $f(\alpha)$ functions (lines) normalized at $\alpha = 0.5$ [$f(\alpha)/f(0.5)$] corresponding to some of the ideal kinetic models included in Table 1 with the reduced Sestak−Berggren function (dots) with the resulting values of n and m coefficients, i.e., $n = 1.081$ and $m = -0.0246$.

this figure (Figure 11) that the kinetic data obtained for the thermal decomposition of $BaCO_3$ perfectly match the F1 kinetic model in agreement with previous references.[33,34] The kinetic parameters obtained here for this material are also coincident with those previously reported by us.[33] Finally, Figure 9 shows that the experimental curves reconstructed from the above kinetic parameters match the TG and SCTA experimental curves, proving the validity of the kinetic parameters calculated by this new kinetic analysis method.

Conclusions

It has been shown that the empirical simplified Sestak−Berggren kinetic equation fits all of the equations corresponding to ideal models proposed for solid-state reactions. Thus, by using the general differential equation (eq 1), which does not have any limitation regarding the heating pathway using for the thermal experiment, and the simplified Sestak−Berggren kinetic equation, a procedure has been proposed for performing the combined kinetic analysis of experimental data obtained under any heating pathway and without any assumptions about the kinetic model fitted by the process. In principle, identical results would be obtained by using another function different from the simplified Sestak−Berggren one with the condition that that equation should perfectly fit all of the equations corresponding to ideal models. The kinetic analysis procedure here proposed has been proved to be quite useful for analyzing not only data obtained under different experimental conditions that fit one of the ideal models proposed in the literature but also processes that cannot be described by one of these models due to deviations produced by effects such as particle size distribution or irregularities in the particles morphologies. The method proposed here has been verified with both theoretical and experimental curves. Thus, different sets of curves simulated by assuming different experimental conditions and/or different deviations from the ideal proposed kinetic models have been analyzed using the combined method proposed here. Additionally, the kinetics of the thermal decomposition of barium carbonate has been studied by the combined analysis of data obtained under linear heating and controlled rate thermal analysis.

Acknowledgment. Financial support was obtained from the Ministry of Education and Science of Spain, Project No. MAT2004-02640 (partially funded by FEDER program).

References and Notes

(1) Galwey, A. K.; Brown, M. E. Kinetic Background to Thermal Analysis and Calorimetry. In *Handbook of Thermal Analysis and Calorimetry*; Brown, M. E., Ed.; Elservier Science: Amsterdam, 1998; Vol. 1 Principles and Practise; p 147.

(2) Galwey, A. K.; Brown, M. E. *Thermal Decomposition of Ionic Solids*; Elsevier: Amsterdam, 1999.

(3) Koga, N.; Tanaka, H. *Thermochim. Acta* **2002**, *388*, 41.

(4) Skrdla, P. J. *J. Phys. Chem. A* **2004**, *108*, 6709.

(5) Budrugeac, P. *Polym. Degrad. Stab.* **2005**, *89*, 265.

(6) Budrugeac, P.; Segal, E.; Perez-Maqueda, L. A.; Criado, J. M. *Polym. Degrad. Stab.* **2004**, *84*, 311.

(7) Burnham, A. K.; Braun, R. L. *Energy Fuels* **1999**, *13*, 1.

(8) Gao, Z. M.; Wang, H. X.; Nakada, M. *Polymer* **2006**, *47*, 1590.

(9) Khawam, A.; Flanagan, D. R. *J. Phys. Chem. B* **2005**, *109*, 10073.

(10) Khawam, A.; Flanagan, D. R. *J. Pharm. Sci.* **2006**, *95*, 472.

(11) Malek, J.; Mitsuhashi, T.; Criado, J. M. *J. Mater. Res.* **2001**, *16*, 1862.

(12) Criado, J. M.; Perez-Maqueda, L. A.; Gotor, F. J.; Malek, J.; Koga, N. *J. Therm. Anal. Calorim.* **2003**, *72*, 901.

(13) Perez-Maqueda, L. A.; Criado, J. M.; Gotor, F. J.; Malek, J. *J. Phys. Chem. A* **2002**, *106*, 2862.

(14) Perez-Maqueda, L. A.; Criado, J. M.; Malek, J. *J. Non-Cryst. Solids* **2003**, *320*, 84.

(15) Svadlak, D.; Shanelova, J.; Malek, J.; Perez-Maqueda, L. A.; Criado, J. M.; Mitsuhashi, T. *Thermochim. Acta* **2004**, *414*, 137.

(16) Cooper, E. A.; Mason, T. O. *J. Am. Ceram. Soc.* **1995**, *78*, 857.

(17) Koga, N.; Criado, J. M. *J. Am. Ceram. Soc.* **1998**, *81*, 2901.

(18) Zhu, Y. T. T.; Stan, M.; Conzone, S. D.; Butt, D. P. *J. Am. Ceram. Soc.* **1999**, *82*, 2785.

(19) Perez-Maqueda, L. A.; Blanes, J. M.; Pascual, J.; Perez-Rodriguez, J. L. *J. European Ceram. Soc.* **2004**, *24*, 2793.

(20) Perez-Maqueda, L. A.; Montes, O. M.; Gonzalez-Macias, E. M.; Franco, F.; Poyato, J.; Perez-Rodriguez, J. L. *Appl. Clay Sci.* **2004**, *24*, 201.

(21) Perez-Rodriguez, J. L.; Pascual, J.; Franco, F.; de Haro, M. C. J.; Duran, A.; del Valle, V. R.; Perez-Maqueda, L. A. *J. Eur. Ceram. Soc.* **2006**, *26*, 747.

(22) Ozawa, T. *Thermochim. Acta* **2000**, *356*, 173.

(23) Reading, M. *J. Therm. Anal. Calorim.* **1998**, *54*, 411.

(24) Reading, M. *J. Therm. Anal. Calorim.* **2001**, *64*, 7.

(25) Criado, J. M.; Perez-Maqueda, L. A. *J. Therm. Anal. Calorim.* **2005**, *80*, 27.

(26) Rouquerol, J.; Sorensen, T. O. General introduction to sample-.controlled thermal analysis (SCTA). In *Sample Controlled Thermal Analysis*; Sorensen, T. O., Rouquerol, J., Eds.; Kluwer: Dordrecht, 2003; p 1.

(27) Ortega, A.; Perez-Maqueda, L. A.; Criado, J. M. *J. Therm. Anal.* **1994**, *42*, 551.

(28) Ortega, A.; Perez-Maqueda, L. A.; Criado, J. M. *Thermochim. Acta* **1994**, *239*, 171.

(29) Ortega, A.; Perez Maqueda, L.; Criado, J. M. *Thermochim. Acta* **1995**, *254*, 147.

(30) Criado, J. M.; Morales, J. *Thermochim. Acta* **1977**, *19*, 305.

(31) Maciejewski, M.; Vyazovkin, S. *Thermochim. Acta* **2001**, *370*, 149.

(32) Sestak, J.; Berggren, G. *Thermochim. Acta* **1971**, *3*, 1.

(33) Perez-Maqueda, L. A.; Criado, J. M.; Gotor, F. I. *Int. J. Chem. Kinet.* **2002**, *34*, 184.

(34) Criado, J. M.; Perez-Maqueda, L. A.; Ortega, A. *J. Therm. Anal.* **1994**, *41*, 1535.